Egypt. J. Chem. **Vol. 68**, No. 11 pp. 529 - 541 (2025)

Egyptian Journal of Chemistry

http://ejchem.journals.ekb.eg/

Chalcones Tethered with Pyridylmethyloxy Tail: Unlocking New Pathways in MDM2-p53 Targeted Cancer Treatment

Suha Alnaeb [1], Mai Adel [1], Maiy Y. Jaballah [1], Nermin Samir [1], Mohamed A. Morsy [2], Khaled A. M. Abouzid [1*]

[1] Department of Pharmaceutical Chemistry, Faculty of Pharmacy, Ain Shams University, Abbassia, Cairo, 11566, Egypt.
[2] Al-Azhar Virology Research Center, Faculty of Medicine, Al-Azhar University, Cairo, 11651, Egypt.

Abstract

The MDM2-p53 pathway has emerged as a pivotal target in cancer research and therapeutic development. Inhibition of MDM2 results in the stabilization and activation of p53, thereby inducing cell cycle arrest and apoptosis in cancer cells that retain wild type p53. Targeting the regulatory mechanisms that govern p53 functionality, especially its interaction with MDM2, represents a promising approach for the development of novel anticancer therapies.

This study focused on the design, synthesis, structural characterization, and biological evaluation of a new series of chalcone-based derivatives incorporating a pyridyl moiety, that aimed at disrupting the p53-MDM2 interaction to exert antiproliferative effects. The synthesized compounds underwent comprehensive *in vitro* evaluation, including cytotoxicity assays, enzyme-linked immunosorbent assays (ELISA), and flow cytometry-based cell cycle analysis, to assess their biological efficacy. Compound **4b** demonstrated potent cytotoxicity in MCF7 (breast cancer) and HepG2 (liver cancer) cell lines, with IC_{50} values of 0.16 µM and 0.17 µM, respectively. Compound **2d** showed moderate activity, particularly against MCF7 cells, with an IC_{50} of 0.21 µM. Additionally, both compounds **4b** and **2d** significantly reduced MDM2 expression by 47% and 36%, respectively, at 10 µM, leading to a corresponding increase in p53 levels by approximately 1.5- and 1.3-fold, respectively, thereby enhancing its tumor-suppressive activity compared to untreated control.

Furthermore, compounds **2d** and **4b**, exhibiting significant biological activity, were evaluated for their effects on cell cycle progression. Both compounds induced a notable depletion in the S phase, suggesting an impact on DNA replication. These results indicate that compound **4b** holds substantial promise for further development as an effective anticancer agent, owing to its potent cytotoxicity across various cancer cell lines and its ability to inhibit MDM2.

Keywords: Synthesis; MDM2; Chalcone; p35; MCF7; Anticancer activity

1. Introduction

Cancer remains the second dominant cause of mortality and morbidity worldwide after cardiac illnesses [1]. According to World Health Organization (WHO) reports, this disease is responsible for almost 10 million fatalities in 2020 and accounts for around one out of every six deaths globally [2]. It is predicted that there will be 29.4 billion cancer patients by 2040, up from 17 million in

2018, underscoring the urgent need for more research, improved therapies and preventive measures [3]. Both internal (hormones, inherited mutations, random mutations and immunological conditions) and external (radiation, mortality, tobacco, infectious organisms and chemicals) factors contribute to cancer [4]. Cancer cells modify a number of important signaling pathways in order to continue dividing by defeating the powerful controls that organize proliferation and cell death in normal cells, and to develop resistance to chemotherapy. These pathways include activating invasion and metastasis, evading growth suppressors, sustaining proliferative signaling, inducing angiogenesis, resisting cell death and enabling replicative immortality [5]. It has long been recognized that p53 is a tumor suppressor protein which acts as the crucial element preventing cancer in humans [6]. P53 has been famously called the “guardian of the genome” because it may react to genotoxic stress, including DNA damage and other stress signals and it can safeguard the genome by triggering several biological reactions, such as DNA repair, apoptosis and cell cycle arrest [7]. In human cancer, the most commonly mutated gene is the tumor suppressor gene TP53 [8,9]. TP53 mutation-induced dysfunctions are closely linked to the tumor formation process [10,11]. The primary role of the p53 protein is that it is a transcription factor, which controls many different processes including autophagy, metabolism, cell cycle arrest, DNA repair, and cell apoptosis [12,13]. When cells are exposed to external and internal stressors, such as hypoxia, nutrient deprivation, DNA damage, p53 ubiquitination is inhibited, which causes intracellular p53 protein levels to rise quickly. Phosphorylation, methylation and acetylation are examples of posttranslational changes that activate and stabilize accumulated p53 [14–17]. In the nucleus, stabilized p53 binds to target DNA creating tetramers and controls gene transcription causing changes in downstream signaling cascades [18–22]. For decades, developing therapies targeting p53 has been difficult because of its unique structure. The p53 protein has a smooth surface without a suitable pocket for drugs to bind effectively, making it

*Corresponding author e-mail: suha.phd2223001@pharma.asu.edu.eg.; (Suha Alnaeb).

Receive Date: 01 February 2025, Revise Date: 28 February 2025, Accept Date: 12 March 2025
DOI: 10.21608/ejchem.2025.356600.11241

hard to design drugs that can restore its function. This structural challenge has significantly hindered progress in creating p53-targeted treatments [23–25], however TP53 is a very attractive target for tumor therapy because of the high prevalence of TP53 mutations in cancers and its intrinsic tumor suppressor role. Activating p53 has been a popular study technique since it involves several candidate compounds that stabilize p53 by preventing it from attaching to mouse double minute 2 (MDM2), an E3 ubiquitin ligase that causes p53 to be degraded by ubiquitination [26–29]. Analogues of nutlin, spirooxindole, isoquilinone, and piperidinone that block the MDM2-p53 interaction are currently showing promise in the treatment of cancer [30]. (Nutlin-3a) **I** with an IC_{50} value of 90 nM is one of the most thoroughly characterized small-molecule inhibitors of the MDM2-p53 interaction. Its clinical development has been limited by suboptimal bioavailability and associated toxicities; however, it remains an indispensable chemical probe for dissecting p53 regulatory pathways [31]. Spirooxindole derivatives are potent MDM2-p53 inhibitors, with (Milademetan) **II** (IC_{50} = 5.57 nM) entering in a first-in-human phase I trial for advanced liposarcoma, solid tumors and lymphomas [32,33]. (NVP-CGM097) **III**, a dihydroisoquinolinone derivative, exhibited strong *in vivo* efficacy and high MDM2 binding affinity (K_i = 1.3 nM) with an IC_{50} value of 1.7 nM [34]. (AM-8553) **IV**, is the first piperidone-based MDM2 inhibitor obtained via structure-based rational design that exhibited an IC_{50} value of 4.2 nM [35,36] **(figure 1)**.

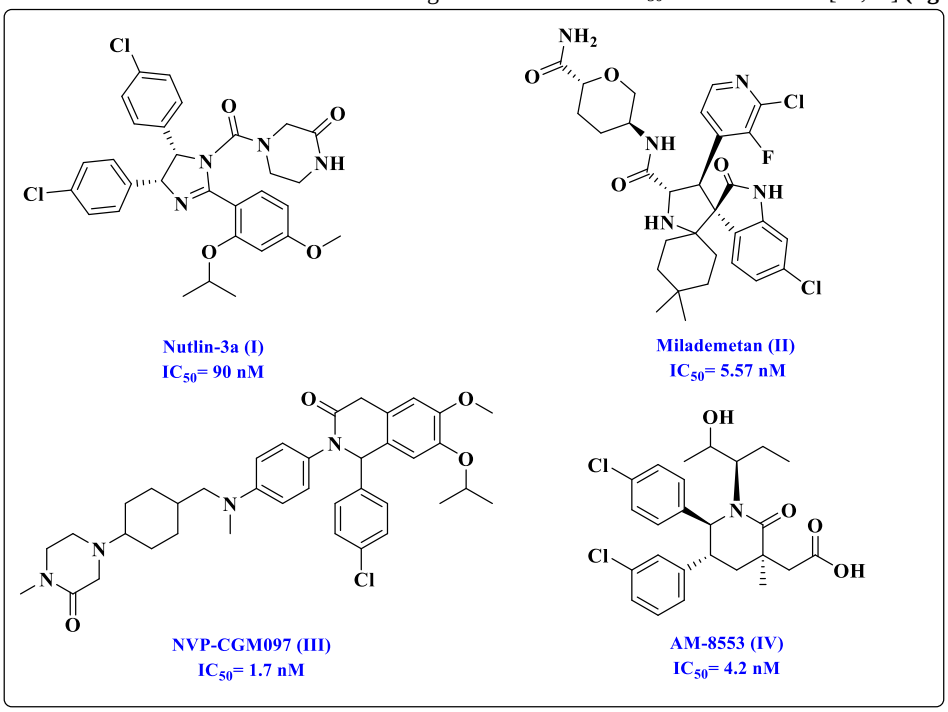

Figure 1: MDM2-p53 inhibitors.

Chalcones, which are the open-chain flavonoids, are a significant class of both synthesized and naturally occurring compounds [37]. Chalcones are made up of two aromatic rings joined by an unsaturated carbonyl system with three carbons (α, β). In medicinal chemistry, chalcones are one of the most advantageous scaffolds which can be easily transformed into a number of heterocyclic scaffolds with therapeutic activity. Antimicrobial [38], antifungal [39], antimalarial [40], anti-inflammatory [41], antileishmanial [42], and anti-tumor properties [43–45]. Some chalcones have been modified with heterocyclic structures and other functional groups to enhance their effectiveness against various targets [46–48]. Tetrahydro-[1,2,4]triazolo[3,4-a]isoquinolin-chalcone derivatives have shown anticancer properties against breast cancer (MCF-7) cells, with compounds **V** and **VI** having IC_{50} values of 50.05 µg/mL and 27.15 µg/mL, respectively [49]. Additionally, a chalcone combined with a thiazole-isoxazole structure compound **VII** demonstrated a promising IC_{50} value of 0.33 ± 0.085 µM against MCF-7 cells [50]. In the same direction thiazole-chalcone hybrids reported by Kasetti exemplified by compound **VIII** showed an IC_{50} value of 6.86 µM against prostate cancer cell line [51]. A group of researchers examined pyridine-chalcone based compounds and compound **IX** (IC_{50}=2.08 µM) exhibited anti-tubulin polymerization activity [52]. Later on, a series of amines-chalcone were synthesized and examined for its antiproliferative activity, where compound **X** was the most effective of all, with IC_{50} values of (8.00, 7.30 and 6.43 µM) for the three cell lines (MDA-MB-231, MDA-MB-468 and MCF-7) respectively [53] **(figure 2)**.

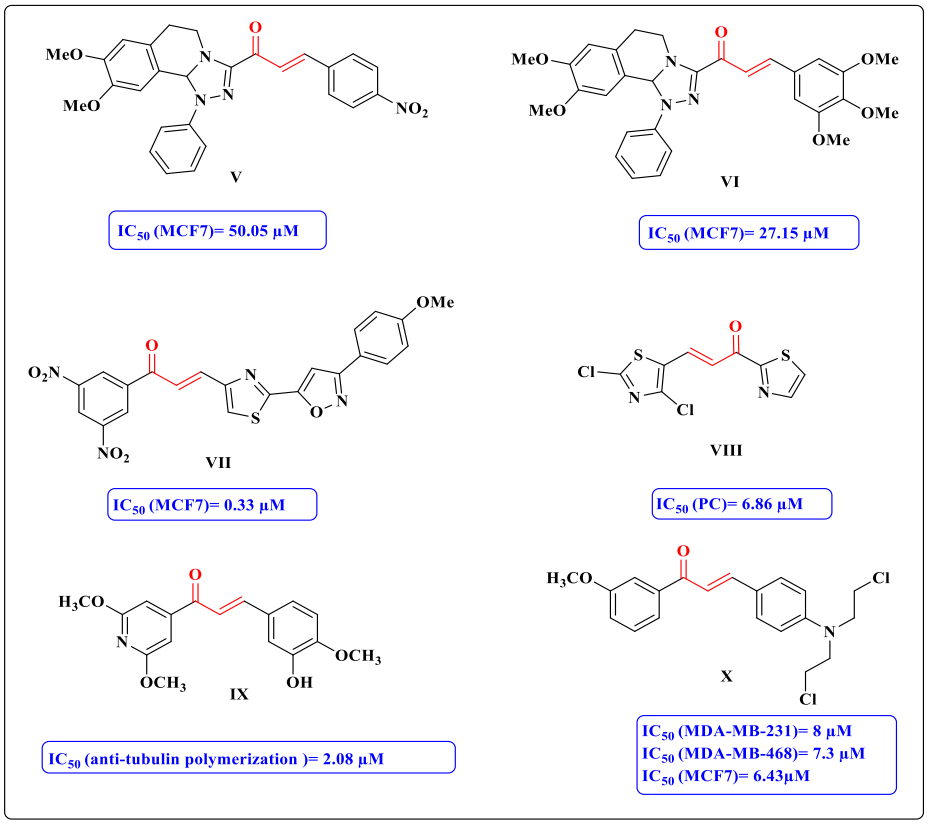

Figure 2: Chalcone-based compounds with anticancer activities.

A series of modified chalcones have been synthesized and evaluated for their ability to stabilize p53 and induce apoptosis in cancer cells. Holak and coworkers have indeed explored the interaction of chalcones with the p53-MDM2 system. Their research demonstrated that chalcones can disrupt the MDM2-p53 interaction. Regarding compound **XI**, an ELISA assay revealed an IC_{50} value of 49 µM [54]. Moreover, to refine target specificity, *Khan et al*. investigated the therapeutic potential of MDM2 inhibition in breast cancer by downregulating its expression using selective boronic-chalcone analogues. They hypothesized that these anti-MDM2 compounds would exert selective antiproliferative effects on breast cancer cells, with compound **XII** exhibited the highest potency, achieving an IC_{50} of 5 µM in wild-type MCF7 cell [55]. Simple chalcones **XIII** and **XIV** were analyzed by immunoblotting method for their activity against p53 in colon cancer cell line and **XIII** showed significant result in inducing the expression of p53 compared to Nutlin-3 [56]. Isoliquiritigenin **XV**, a bioactive flavonoid isolated from liquorice roots and shallot, demonstrated significant anticancer potential. It has been reported to induce cell cycle arrest and apoptosis in liver cancer cells via p53 pathway activation at concentrations ranging from 10 to 20 µg/mL. However, its binding affinity and interaction with MDM2 remain uncharacterized [55,57] **(figure 3)**.

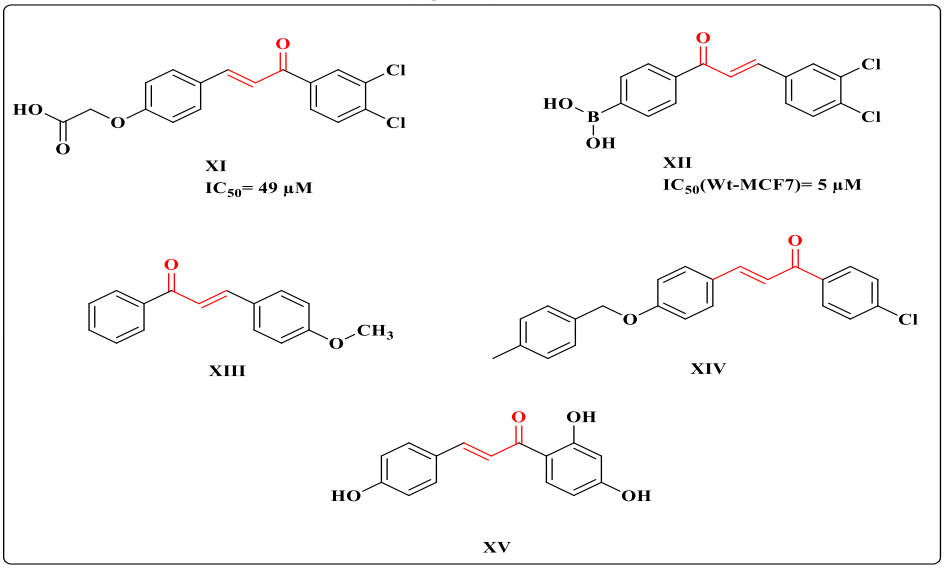

Figure 3: Chalcone- based compounds as MDM2-p53 inhibitors**.**

Generally, there are different methods for the synthesis of chalcones such as aldol reaction, Claisen-Schmidt's condensation, coupling reactions, continuous-flow deuteration reaction and solid acid catalyst-mediated reaction [58]. In this study, Claisen-Schmidt's condensation reaction between a ketone having α-hydrogen with an aromatic carbonyl compound in the presence of a base or an acid was utilized for the synthesis of the target chalcones [59–61]. This method promotes the high-yield production of the (*E*)-isomer [62].

Our design approach was guided by previously reported chalcone-based compounds with MDM2 inhibitory properties, as well as several heterocyclic structures exhibiting notable anticancer activity. Based on these precedents, we shifted our focus to the development of pyridine-chalcone-based compounds. We employed a hybridization strategy by combining compound **XIV** with compound **IX**, resulting in a library of ten chalcones **(series 1 and 2)**, each incorporating various functional groups such as fluoro, bromo, methoxy, and chloro which can either donate or withdraw electrons on a single phenyl ring **(Figure 4)**. These chalcones feature varying molecular lengths and degrees of electron density in the aromatic ring. Additionally, we investigated the influence of alternating the ketone group with the double bond on p53 stabilization. Our evaluation also aimed to determine whether these chalcones could stabilize p53, offering valuable insights for further structural optimization and modifications.

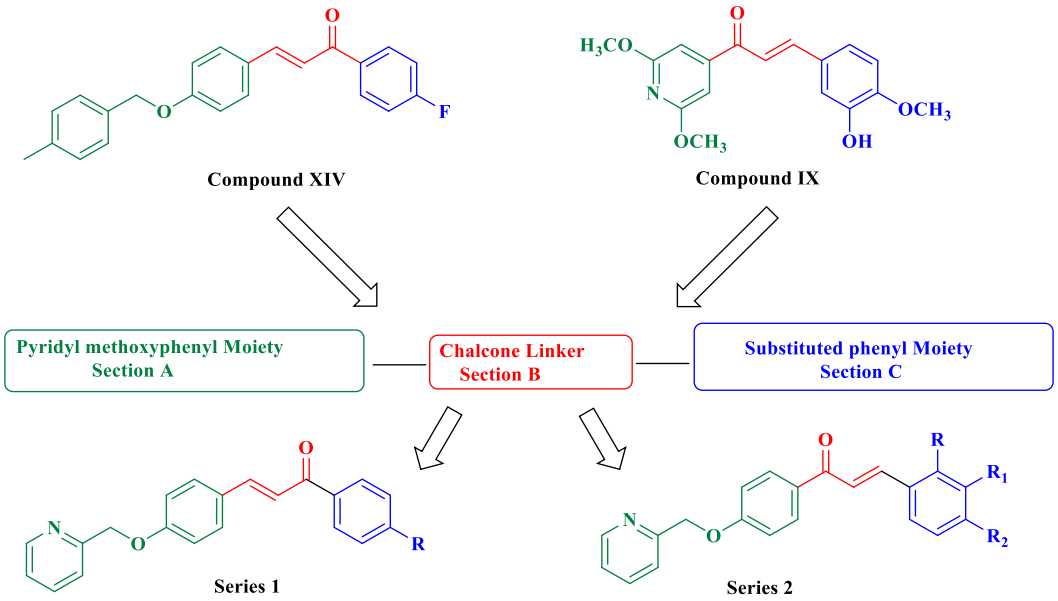

Figure 4: Rational design of the target chalcones through molecular hybridization strategy**.**

2. Experimental (Materials and Methods)

2.1. Chemistry:

Starting materials, reagents and solvents obtained from available sources and used without further purification. Reactions were monitored by analytical thin layer chromatography (TLC), performed on silica gel 60 F254 packed on Aluminum sheets, purchased from Merck. Melting points were recorded on Stuart Scientific apparatus. The HRMS were recorded on LC/Q-TOF, 6530 (Agilent Technologies, Santa Clara, CA, USA) at Natural product research lab, Faculty of pharmacy, Fayoum University. ^{1}HNMR and ^{13}CNMR spectra were recorded on a Bruker Advance III HD FT-high resolution- NMR 400 MHz and scaled as δ in ppm at center of drug discovery, Faculty of pharmacy, Ain shams University.

2.1.1. 4-(Pyridin-2-ylmethoxy) benzaldehyde (1)

To a solution of 4-hydroxybenzaldehyde (0.446 g, 3.66 mmol, 1.2 eq) in dry acetonitrile (20 mL), anhydrous K_2CO_3 (0.84g, 6.07 mmol, 2 eq) was added. The reaction mixture was stirred for 30 min and 2-chloromethylpyridine hydrochloride (0.5 g, 3.05 mmol, 1 eq) was added and stirring was continued 12 h at reflux temperature. The reaction was monitored by TLC. After the completion of the reaction, the solvent was evaporated under reduced pressure. The formed solid was filtered, washed with water to yield the titled compound **(1)** as white solid; yield (83%); m.p. 94-97 °C.

2.1.2. General procedure for the synthesis of chalcones (2a-d)

Appropriate acetophenone (0.93 mmol, 1 eq) was dissolved in ethanol (5 mL) then 10% KOH (1 mL) was added dropwise and stirred for 30 min at room temperature. Compound **(1)** (0.93 mmol, 1 eq) was dissolved in 5 mL of ethanol and then was added to the previous solution with stirring. The reaction was stirred at room temperature for 24 h. After completion of the reaction, the mixture was poured into ice water, acidified with 10% aqueous hydrochloric acid. The formed solid was filtered under vacuum, washed with water and ethanol and then purified by recrystallization in ethanol to give the designed compounds (**2a-d).**

2.1.2.1. *(E)*-1-Phenyl-3-(4-(pyridin-2-ylmethoxy) phenyl) prop-2-en-1-one (2a).
White solid; yield (65%); m.p. 100-102 °C; **^{1}H NMR (400 MHz, DMSO)** δ 8.63 – 8.57 (m, 1H), 8.14 (d, *J*=12 Hz, 2H), 7.91 – 7.77 (m, 4H), 7.77 – 7.62 (m, 2H), 7.61 – 7.51 (m, 3H), 7.40 – 7.32 (m, 1H), 7.13 (d, *J*=12 Hz, 2H), 5.27 (s, 2H).; **HRMS** (ESI) m/z $[M + H]^+$ calcd. for **$C_{21}H_{17}NO_2$**: 316.1337, **found** 316.13422.

2.1.2.2. *(E)*-1-(4-Chlorophenyl)-3-(4-(pyridin-2-ylmethoxy) phenyl) prop-2-en-1-one (2b).
White solid; yield (70%); m.p. 148-150 °C; **^{1}H NMR (400 MHz, DMSO)** δ 8.60 (d, *J* = 4.9 Hz, 1H), 8.16 (d, 2H), 7.90 – 7.77 (m, 4H), 7.73 (d, *J* = 15.6 Hz, 1H), 7.63 (d, 2H), 7.54 (d, *J* = 7.9 Hz, 1H), 7.36 (dd, *J* = 7.6, 4.9 Hz, 1H), 7.12 (d, 2H), 5.27 (s, 2H).; **HRMS** (ESI) m/z $[M + H]^+$ calcd. for **$C_{21}H_{16}ClNO_2$**: 350.0948, **found** 350.09559 and 352.09324.

2.1.2.3. *(E)*-1-(4-Bromophenyl)-3-(4-(pyridin-2-ylmethoxy) phenyl) prop-2-en-1-one (2c).
White solid; yield (66%); m.p. 148-150 °C; **^{1}H NMR (400 MHz, DMSO)** δ 8.60 (dt, *J* = 4.7, 1.5 Hz, 1H), 8.08 (d, *J* = 9.4 Hz, 2H), 7.91 – 7.69 (m, 7H), 7.54 (d, *J* = 7.8 Hz, 1H), 7.36 (ddd, *J* = 7.5, 4.9, 1.2 Hz, 1H), 7.17 – 7.08 (d, *J* = 8.5 Hz, 2H), 5.27 (s, 2H); **HRMS** (ESI) m/z $[M + H]^+$ calcd. for **$C_{21}H_{16}BrNO_2$**: 394.0442, **found** 394.04501 and 396.04327.

2.1.2.4. *(E)*-1-(4-Methoxyphenyl)-3-(4-(pyridin-2-ylmethoxy) phenyl) prop-2-en-1-one (2d).
White solid; yield (65%); m.p. 98-100 °C; **^{1}H NMR (400 MHz, DMSO)** δ 8.72 – 8.48 (m, 1H), 8.16 (d, *J* = 8.4 Hz, 2H), 7.90 – 7.77 (m, 4H), 7.68 (d, *J* = 15.5 Hz, 1H), 7.54 (d, *J* = 7.8 Hz, 1H), 7.36 (ddd, *J* = 7.6, 4.8, 1.2 Hz, 1H), 7.16 – 7.04 (m, 4H), 5.26 (s, 2H), 3.87 (s, 3H); **^{13}C NMR (101 MHz, DMSO)** δ 187.77, 163.56, 160.52, 156.81, 149.63, 143.45, 137.50, 131.26, 131.13, 128.32, 123.54, 122.27, 120.23, 115.68, 114.44, 70.89, 56.01; **HRMS** (ESI) m/z $[M + H]^+$ calcd. for **$C_{22}H_{19}NO_3$**: 346.1443, **found** 346.14466.

2.1.3. 1-(4-(Pyridin-2-ylmethoxy) phenyl) ethan-1-one (3)
To a solution of 4-hydroxyacetophenone (1 g, 7.3 mmol, 1.2 eq) in dry acetonitrile (20 mL), anhydrous K_2CO_3 (1.68 g, 12.15 mmol, 2 eq) was added. The reaction mixture was stirred for 30 min and 2-chloromethylpyridine hydrochloride (1 g, 6.09 mmol, 1 eq) was added and stirring was continued 12 h at reflux temperature. The reaction was monitored by TLC. After the completion of the reaction, the solvent was evaporated under reduced pressure. The formed solid was filtered, washed with water to yield the titled compound **(3)** as white solid; yield (93%); m.p. 100-102 °C.

2.1.4. General procedure for the synthesis of chalcones (4a-f)
Compound **(3)** (0.88 mmol, 1 eq) was dissolved in ethanol (5mL), then 10% KOH (1mL) was added dropwise and stirred for 30 min at room temperature. Appropriate benzaldehyde (0.88 mmol, 1 eq) was dissolved in 5 mL of ethanol then added to the previous solution with stirring. The reaction was stirred at room temperature for 24 h. After completion of the reaction, the mixture was poured into ice water, acidified with 10% aqueous hydrochloric acid. The formed solid was filtered under *vacuum*, washed with water and ethanol and then purified by recrystallization in ethanol to give the designed compounds **(4a-f)**.

2.1.4.1 *(E)*-3-(4-Chlorophenyl)-1-(4-(pyridin-2-ylmethoxy) phenyl) prop-2-en-1-one (4a).
White solid; yield (68%); m.p. 180-182 °C; **^{1}H NMR (400 MHz, DMSO)** δ 8.64 – 8.57 (m, 1H), 8.18 (d, *J* = 8.8 Hz, 2H), 7.97 (d, *J* = 15.6 Hz, 1H), 7.93 (d, *J* = 8.4 Hz, 2H), 7.86 (td, *J* = 7.7, 1.8 Hz, 1H), 7.70 (d, *J* = 15.6 Hz, 1H),), 7.59 – 7.47 (m, 3H), 7.37 (dd, *J* = 7.5, 4.9 Hz, 1H), 7.19 (d, *J* = 8.7 Hz, 2H), 5.32 (s, 2H); **HRMS** (ESI) m/z $[M + H]^+$ calcd. for **$C_{21}H_{16}ClNO_2$**: 350.0948, **found** 350.09551 and 352.09326.

2.1.4.2. *(E)*-3-(4-Fluorophenyl)-1-(4-(pyridin-2-ylmethoxy) phenyl) prop-2-en-1-one (4b).
White solid; yield (66%); m.p. 150-152 °C; **^{1}H NMR (400 MHz, DMSO)** δ 8.60 (d, *J* = 4.8 Hz, 1H), 8.18 (d, *J* = 8.5 Hz, 2H), 8.01 – 7.87 (m, 3H), 7.85 (t, *J* = 7.7 Hz, 1H), 7.71 (d, *J* = 15.5 Hz, 1H), 7.55 (d, *J* = 7.9 Hz, 1H), 7.37 (t, *J* = 6.4 Hz, 1H), 7.30 (t, *J* = 8.8 Hz, 2H), 7.19 (d, *J* = 8.4 Hz, 2H), 5.32 (s, 2H); **^{13}C NMR (101 MHz, DMSO)** δ 187.75, 165.02, 162.58, 156.58, 149.67, 142.43, 137.51, 131.98, 131.63, 131.54, 131.42, 131.23, 123.59, 122.37, 122.30, 116.45, 116.24, 115.30, 71.02; **HRMS** (ESI) m/z $[M + H]^+$ calcd. for **$C_{21}H_{16}FNO_2$**: 334.1243, **found** 334.12493.

2.1.4.3. *(E)*-3-(4-Bromophenyl)-1-(4-(pyridin-2-ylmethoxy) phenyl) prop-2-en-1-one (4c).
White solid; yield (72%); m.p. 180-182 °C; **^{1}H NMR (400 MHz, DMSO)** δ 8.60 (d, *J* = 4.9 Hz, 1H), 8.18 (d, *J* = 8.3 Hz, 2H), 7.98 (d, *J* = 15.6 Hz, 1H), 7.85 (d, *J* = 7.4 Hz, 3H), 7.72 – 7.59 (m, 3H), 7.55 (d, *J* = 7.9 Hz, 1H), 7.41 – 7.34 (m, 1H), 7.19 (d, *J* = 8.2 Hz, 2H), 5.32 (s, 2H); **HRMS** (ESI) m/z $[M + H]^+$ calcd. for **$C_{21}H_{16}BrNO_2$**: 394.0442, **found** 394.04495 and 396.04316.
2.1.4.4. *(E)*-3-(4-Methoxyphenyl)-1-(4-(pyridin-2-ylmethoxy) phenyl) prop-2-en-1-one (4d).
White solid; yield (60%); m.p. 132-134 °C; **^{1}H NMR (400 MHz, DMSO)** δ 8.64 – 8.57 (d, 1H), 8.16 (d, *J* = 8.8 Hz, 2H), 7.89 – 7.77 (m, 4H), 7.69 (d, *J* = 15.5 Hz, 1H), 7.55 (d, *J* = 7.8 Hz, 1H), 7.41 – 7.33 (m, 1H),), 7.18 (d, *J* = 8.2 Hz, 2H), 7.02 (d, *J* = 8.8 Hz, 2H), 5.32 (s, 2H), 3.83 (s, 3H); **HRMS** (ESI) m/z $[M + H]^+$ calcd. for **$C_{22}H_{19}NO_3$**: 346.1443, **found** 346.14491.

2.1.4.5. *(E)*-3-(2-Chlorophenyl)-1-(4-(pyridin-2-ylmethoxy) phenyl) prop-2-en-1-one (4e).
White solid; yield (62%); m.p. 108-110 °C; **^{1}H NMR (400 MHz, DMSO)** δ 8.64 – 8.57 (m, 1H), 8.25 – 8.15 (m, 3H), 8.01 (d, *J* = 1.7 Hz, 2H), 7.86 (td, *J* = 7.7, 1.8 Hz, 1H), 7.61 – 7.52 (m, 2H), 7.47 (tt, *J* = 7.3, 5.3 Hz, 2H), 7.37 (dd, *J* = 7.6, 5.0 Hz, 1H), 7.25 – 7.17 (m, 2H), 5.33 (s, 2H); **HRMS** (ESI) m/z $[M + H]^+$ calcd. for **$C_{21}H_{16}ClNO_2$**: 350.0948, **found** 350.09582 and 352.09343.

2.1.4.6. *(E)*-3-(4-Chloro-3-fluorophenyl)-1-(4-(pyridin-2-ylmethoxy) phenyl) prop-2-en-1-one (4f).
White solid; yield (65 %); m.p. 180-182 °C; **^{1}H NMR (400 MHz, DMSO)** δ 8.61 (d, *J* = 4.6 Hz, 1H), 8.20 (d, *J* = 8.8 Hz, 2H), 8.12 – 8.00 (m, 2H), 7.86 (td, *J* = 7.7, 1.8 Hz, 1H), 7.74 (dd, *J* = 8.4, 1.9 Hz, 1H), 7.72 – 7.63 (m, 2H), 7.56 (d, *J* = 7.8 Hz, 1H),

7.38 (dd, *J* = 7.6, 4.9 Hz, 1H), 7.24 – 7.16 (m, 2H), 5.33 (s, 2H); **HRMS** (ESI) m/z $[M + H]^+$ calcd. for **$C_{21}H_{15}ClFNO_2$**: 368.0853, **found** 368.08592 and 370.08395.

2.2. Biology:

2.2.1. Anticancer activity:

2.2.1.1. Reagents and Chemicals:

RPMI 1640, (FBS), trypsin and (PBS) were purchased from (ICN Biomedicals Inc. 1263 south Chillicothe Ohio, USA). MTT was obtained from (YUNBANG PHARMA, Cas no. 298-93-1, China) and penicillin/streptomycin from Invitrogen (San Diego, CA, USA). Doxorubicin and DMSO were obtained from EBEWE Pharma (Unterach, Austria) and Merck (Darmstadt, Germany), respectively. All biology tests were conducted in (Microbiology department, faculty of medicine Al-Azhar University, Cairo, Egypt).

2.2.1.2. Cell culture:

Six human cell lines (HCT-116, A-549, K-562, PC3, HepG2, MCF7) and a normal human embryonic kidney cell line (HEK-293) were obtained from (Microbiology department, faculty of medicine Al-Azhar University, Cairo, Egypt). All cell lines were marinated in RPMI 1640 supplemented with 10% FBS, streptomycin (100 µg/mL) and penicillin-G (100 units/mL). Cells were grown in monolayer cultures.

2.2.1.3. Cytotoxicity assay:

Cell viability following exposure to the synthetic compounds was estimated using MTT assay [63]. Cells were plated in 96-well microplates at a density of 1 × 104 (8000- 10000) cells per well (100 µL per well). Control wells contained no drugs and blank wells contained only growth medium for background correction. After cell attachment, the medium was removed, and cells were incubated with a serum-free medium containing 10000 µg/mL of the synthetic compounds by 1/2 serial dilutions. Compounds were all first dissolved in DMSO and then diluted in medium, therefore the maximum concentration of DMSO in the wells did not exceed 0.5%. Cells were further incubated for 24 h. At the end of the incubation time, the medium was removed and MTT solution was added to each well at a final concentration of 5 mg/mL and plates were incubated for another 4 h at 37 °C. Then formazan crystals were solubilized in 150 µL DMSO. The optical density was measured at 570 nm with background correction at 655 nm using a (STAT-fax 2100) microplate reader (Serial 2100-4019, UK). The percentage of inhibition of viability compared to control wells was calculated for each concentration of the compound and IC_{50} values were calculated with Graphprism Ver. 9. Each experiment was carried out in triplicate.

2.2.1.4. *In vitro* Enzyme-Linked Immunosorbent Assay (ELISA)

2.2.1.4.1. Measuring MDM2-p53 Binding Protein Homolog (MDM2)

Human MDM2 assay kit (cat. ELK4557 **ELKbiotech, USA**) was used and the experimental protocol was done according to manufacturer. The microtiter plate provided has been pre-coated with an antibody specific to MDM2. Standards or samples are then added to the appropriate microtiter plate wells with a biotin-conjugated antibody specific to MDM2. Next, Avidin conjugated to Horseradish Peroxidase (HRP) is added to each microplate well and incubated. After TMB substrate solution. is added, only those wells that contain MDM2, biotin-conjugated antibody and enzyme-conjugated Avidin will exhibit a change in color. The enzyme-substrate reaction is terminated by the addition of sulphuric acid solution and the color change is measured spectrophotometrically at a wavelength of 450nm ± 10nm. The concentration of MDM2 in the samples is then determined by comparing the O.D. of the samples to the standard curve. All reagents, samples and standards are prepared. 100µL standard or sample were added to each well and incubated for 80 minutes at 37ºC. 100µL of the Biotinylated Antibody Working Solution was added and incubated for 50 minutes at 37ºC. 100µL of the Streptavidin-HRP Working Solution was added and incubated for 50 minutes at 37ºC. 90µL of TMB Substrate solution was added and incubated for 20 minutes at 37ºC. Finally, 50µL Stop Solution were added and read at 450 nm immediately. Each experiment was carried out in triplicate.

2.2.1.4.2. Measuring the Tumour Protein p53 Binding Protein (TP53)

Human TP53 assay kit (cat. ELK1507 **ELKbiotech, USA**) was used and the experimental protocol was done according to manufacturer. The microplate provided has been pre-coated with an antibody specific to TP53. Standards or samples are then added to the appropriate microplate wells with a biotin-conjugated antibody specific to Human TP53. Next, Avidin conjugated to Horseradish Peroxidase (HRP) is added to each microplate well and incubated. After TMB substrate solution is added, only those wells that contain Human TP53, biotin-conjugated antibody and enzyme-conjugated Avidin will exhibit a change in colour. The enzyme-substrate reaction is terminated by the addition of sulphuric acid solution and the colour change is measured spectrophotometrically at a wavelength of 450nm ± 10nm. The concentration of Human TP53 in the samples is then determined by comparing the O.D. of the samples to the standard curve. All reagents, samples and standards were prepared, 100 µL of standard or sample were added to each well. After 80 minutes incubation at 37ºC; add 100 µL Biotinylated Antibody Working Solution for 50 minutes at 37ºC then 100 µL of the Sreptavidin-HRP Working Solution was incubated at 37ºC for 50 minutes. 90µL of TMB Substrate Solution was added and incubated for 20 minutes at 37ºC. Finally, 50µL of Stop Solution were added and absorbance was read at 450nm immediately. Each experiment was carried out in triplicate.

2.2.1.4. *In vitro* cell cycle analysis by flowcytometry

Cell cycle analysis by flowcytometry was conducted for the chalcone compounds **2d** and **4b** due to its wide anticancer spectrum, at Creative Egyptian Biotechnologists company (CEB), Dokki, Giza, Egypt.

Analysis of Cell Cycle Distribution

After treatment with test compounds and MCF7 (as control) for 24 h, cells (10^6 cells) are collected by trypsinization and washed twice with ice-cold PBS (pH 7.4). Cells are re-suspended in two milliliters of 60% ice-cold ethanol and incubated at 4ºC for 1 h for fixation. Fixed cells are washed twice again with PBS (pH 7.4) and resuspended in 1 mL of PBS containing 50 µg/mL RNAase A and 10 µg/mL propidium iodide (PI). After 30 min of incubation in dark at 15-25ºC, cells are analyzed for DNA contents using flowcytometry analysis using FL2 (λex/em 535/617 nm) signal detector (Cytoflex™ flowcytometer, cytexpert software, from Beckman Coulter, ACEA Biosciences, USA). For each sample, 20,000 events minimum are acquired. Cell cycle distribution is calculated using Cytexpert™ software (Beckman Coulter ACEA, USA).

3. Results and Discussion

3.1. Chemistry:

The targeted compounds **(2a-d)** were synthesized by reacting ortho chloromethyl pyridine with para hydroxy benzaldehyde in acetonitrile in the presence of potassium carbonate at reflux for 12 h [64]. Removal of the solvent yielded the desired intermediate [4-(pyridin-2-ylmethoxy) benzaldehyde] which was then reacted through Claisen-Shmidt condensation reaction with the appropriate acetophenone in ethanol using 10% potassium hydroxide at room temperature to afford chalcones (**scheme 1**) [65,66]. Whereas compounds **(4a-f)** (**scheme 2**) were synthesized by reacting ortho chloromethyl pyridine with para hydroxy acetophenone in acetonitrile to obtain the ketone intermediate [1-(4-(pyridin-2-ylmethoxy) phenyl) ethan-1-one] [64] which was then reacted with the appropriate benzaldehyde to obtain the desired compounds [65,66]. The structures were confirmed using ^{1}H NMR, ^{13}C NMR, and HRMS, and the yields ranged from 60% to 72%.

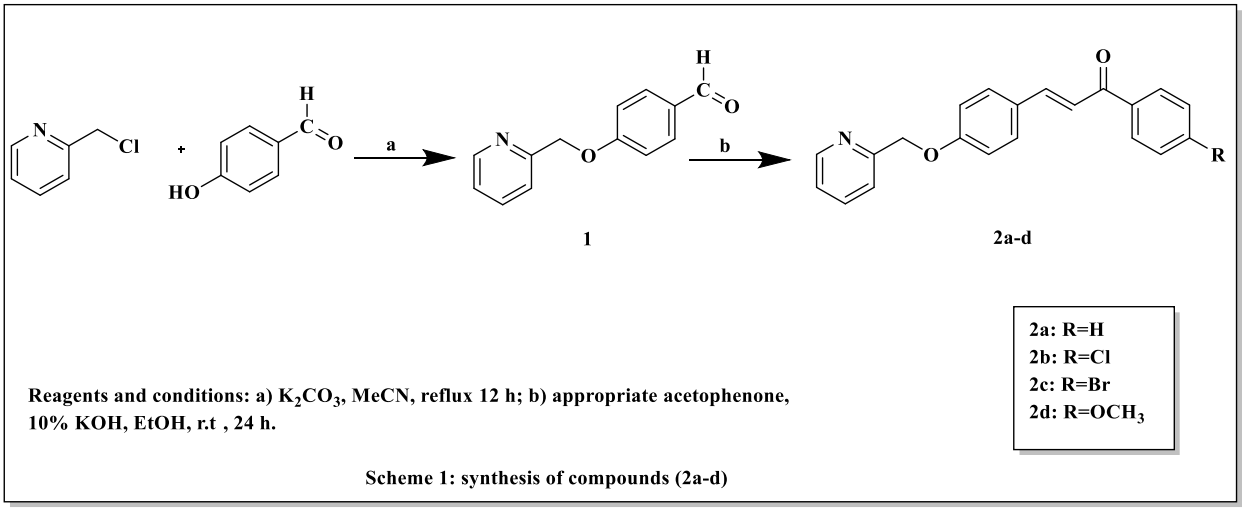

Scheme 1: synthesis of compounds (2a-d)

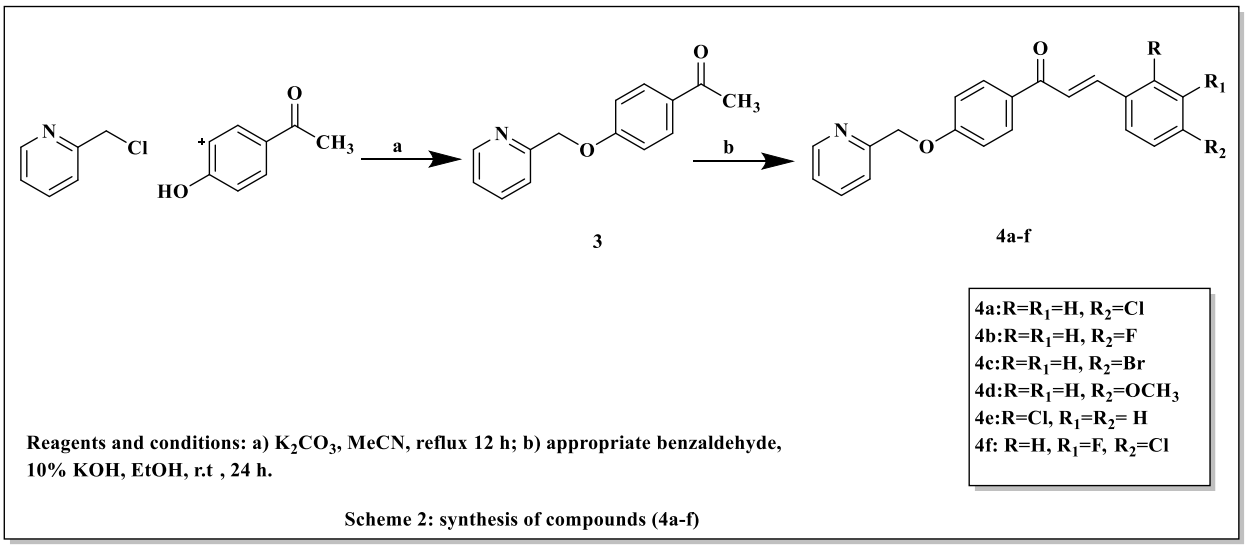

Scheme 2: synthesis of compounds (4a-f)

3.2. Biology

3.2.1. *In vitro* cytotoxic activity assay against (MCF7, HepG2, PC3, A549, HCT-116, and k-562) cell lines.

Cytotoxic activity was estimated for the ten synthesized compounds on six cell lines (MCF7, HepG2, PC3, A549, HCT-116, and k-562) and one normal human embryonic kidney cell line (HEK-293) compared with doxorubicin as a control. While the majority of the compounds exhibited modest antiproliferative activity against the mentioned cell lines, MCF7 and HepG2 cell

lines were the most sensitive cell line to our compounds. Data analysis showed that compound **4b** demonstrated significant anticancer activity against most of the tested cell lines especially liver cancer (HepG2), and breast cancer (MCF7) with IC_{50} (0.17, 0.16 µM) respectively, and with low cytotoxicity against normal cell line IC_{50} (1.32 µM) compared to doxorubicin IC_{50} (0.13 µM). Whereas compound **2d** showed moderate antiproliferative activity against the MCF7 cell line with IC_{50} (0.21 µM). The results showed that switching the position of the carbonyl group and double bond had an impact on the cell lines' effectiveness when comparing substances **2b** IC_{50} (0.5 µM) with **4a** IC_{50} (0.37 µM) and **2c** IC_{50} (0.57 µM) with **4c** IC_{50} (0.38 µM) on the MCF7 cell line. Analysis of compounds **4a** (IC_{50}= 0.37 µM) and **4e** (IC_{50}= 0.33 µM) showed that the efficacy on the MCF7 cell line remained relatively unaffected. This indicates that the position of the halogen (whether para or ortho) in the phenyl group did not significantly impact the activity. The MCF7 cell line is well-known for being both estrogen receptor (ER) positive and progesterone receptor (PR) positive and it contains the wild-type p53 gene. The pronounced overexpression of MDM2 in these cells renders them a suitable model for dissecting the molecular mechanisms governing MDM2-p53 inhibition. Thus, this cell line was selected to systematically investigate the impact of compounds **2d** and **4b** on the suppression of the MDM2-p53 interactions [32,67] **(Table 1)**.

Table 1. IC_{50} values of target compounds on seven cell lines.

Compound ID	IC_{50} µM						
	HCT-116	A-549	K-562	PC3	HepG2	MCF7	HEK-293 (normal cell line)
2a	0.55	0.21	0.39	0.37	0.70	0.28	0.58
2b	0.62	0.57	1.91	0.61	0.17	0.50	1.16
2c	1.03	0.35	1.17	0.54	0.32	0.57	0.20
2d	0.75	0.32	1.41	0.63	0.61	**0.21**	0.25
4a	0.35	0.60	0.55	0.60	0.61	0.37	0.42
4b	0.18	0.17	0.28	0.50	**0.17**	**0.16**	**1.32**
4c	0.32	1.31	3.18	0.94	0.64	0.38	1.01
4d	2.17	0.68	1.03	0.37	0.45	0.86	0.43
4e	0.62	0.46	2.03	0.67	0.22	0.33	0.49
4f	0.53	0.56	0.71	1.23	1.18	0.29	1.59
Doxorubicin	0.06	0.05	0.13	0.01	0.15	**0.10**	**0.13**

3.2.2. *In vitro* Enzyme-Linked Immunosorbent Assay (ELISA) assay

3.2.2.1. Measuring MDM2-p53 Binding Protein Homolog (Human MDM2)

The most potent compound on the MCF7 cell line from each scheme was chosen for screening at five doses of concentrations (0.625, 1.25, 2.5, 5, 10 µM) to test their activity as MDM2 inhibitors (**Figure 5**). An ELISA-based assay was employed to determine the MDM2 protein concentration (ng/mL) in the MCF7 breast cancer cell line. The inhibitory potential of compounds **2d** and **4b** on MDM2 protein was quantitatively assessed by calculating the percentage of activity suppression relative to untreated MCF7 cells. The tested compounds showed moderate inhibitory activity against MDM2. Compound **4b** showed inhibitory activity of 47% against MDM2 at 10 µM concentration compared to **2d** compound that showed 36% inhibitory activity.

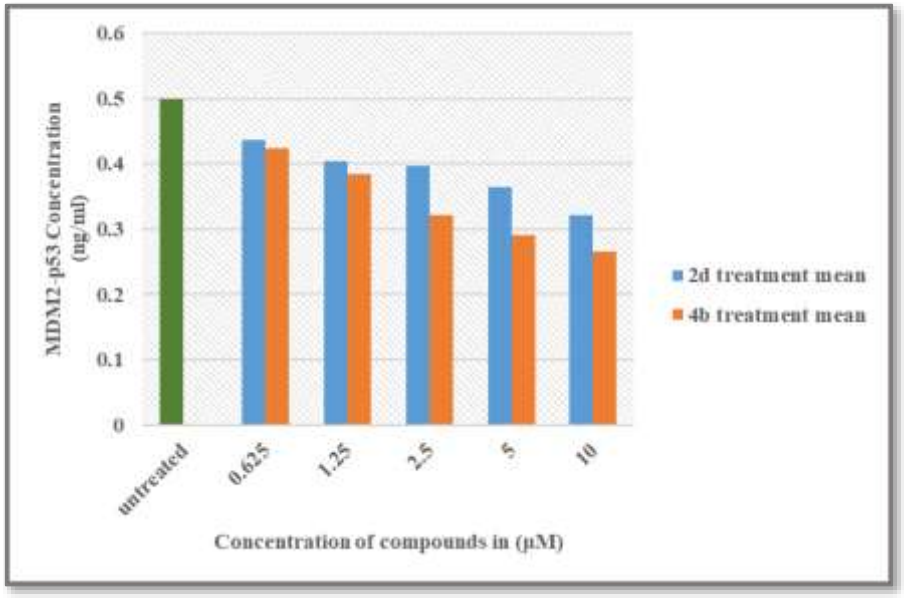

Figure 5: Effect of compounds 2d and 4b on the MDM2 expression in MCF7 cell line quantified by ELISA.

3.2.2.2. Measuring the Tumour Protein p53 Binding Protein (TP53)

When the MDM2-p53 interaction is disrupted, p53 levels rise and transcriptional activity of p53 is restored, suggesting that the genome integrity check has been restored and that MDM2-p53 binding antagonists have therapeutic promise. Depending on the previous fact, ELISA was utilized to determine the p53 protein concentration (pg/mL) in MCF7 breast cancer cells following treatment with compounds **2d** and **4b** at varying concentrations (0.625, 1.25, 2.5, 5, and 10 µM). The findings demonstrated a significant upregulation of p53 protein expression at 10 µM, exhibiting an approximately 1.3- to 1.5-fold increase relative to untreated MCF7 cells **(figure 6)**.

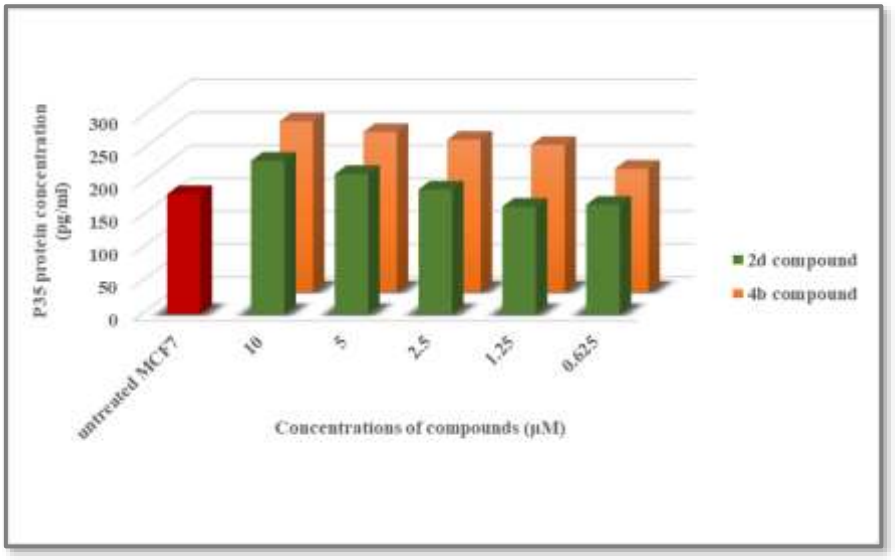

Figure 6: Effect of compounds 2d and 4b on the p53 expression in MCF7 cell line quantified by ELISA.

3.2.3. *In vitro* cell cycle analysis by flowcytometry

The cell cycle is a sequence of events that includes DNA replication, cell division, and ultimately the production of two daughter cells [68]. To reduce a chance of nonspecific drug side effects during cancer treatment, it is attractive to build new anti-proliferative drugs that can regulate cell cycle progression and death. Consequently, the most effective anticancer substance **2d** and **4b**, which showed notable activity on the MCF7 cell line, were also chosen for more research into their ability to induce cell cycle arrest. Compounds **2d** and **4b** arrested the cell cycle at the S and G2/M phase, where the cell population levels of p53 wild-type cell lines MCF7 were decreased from (24.74, 6.48%) for the control to (15.34, 2.59%) and (17.92, 2.28%) for **2d** and **4b** respectively. However, the two examined compounds exhibited an additional arrest to the G0-G1 phase of the cell cycle which increased the cell population levels of the two examined compounds (82.07, 79.79%) respectively, compared to the control (68.79%) (**Figures 7 and 8**).

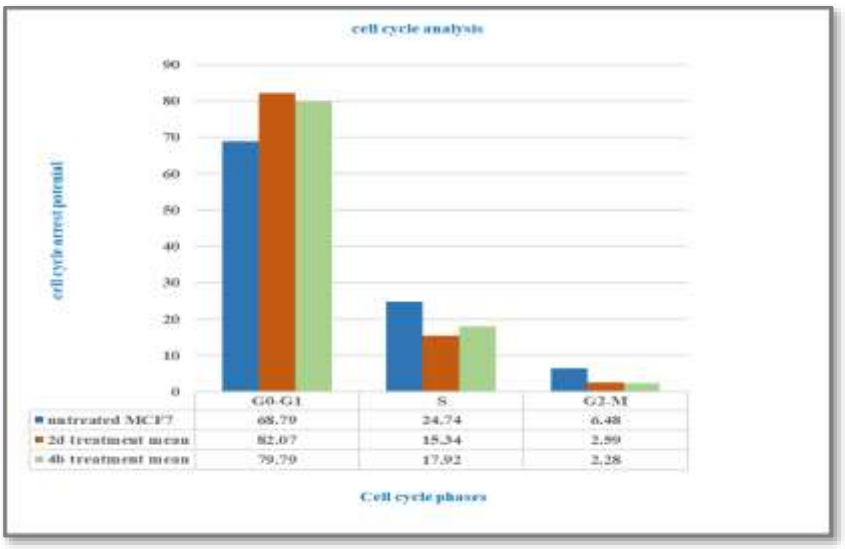

Figure 7: Cell cycle analysis for MCF7 cell line after treatment with 2d and 4b compounds.

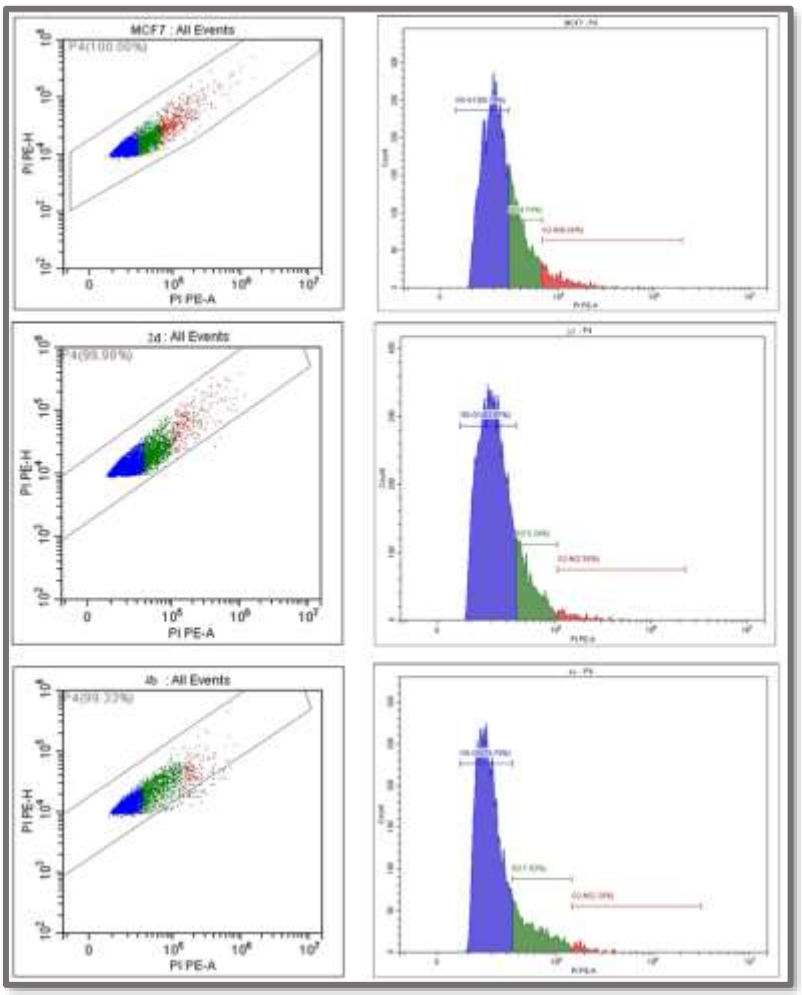

Figure 8: Histograms of the cell cycle for control and compounds 2d and 4b in MCF7 cell line.

4. Conclusion

New chalcone-based derivatives were synthesized and assessed *in vitro* for their anticancer activity, against six cancer cell lines (MCF7, HepG2, PC3, A549, HCT-116, and k-562) and one normal (HEK-293) cell line. Significant antiproliferative activity was demonstrated by the compounds **2d** and **4b** against the MCF7 cell line (IC_{50} = 0.21, 0.16 µM) respectively. The switching between carbonyl group and double bond in the pyridine chalcone derivatives played a role in increasing the anticancer activity against the majority of cell lines as proved by the notable antiproliferative activity of compound **4b**. Compounds **2d** and **4b** were tested for their effects on MDM2 at concentration of 10 µM and they showed 36 and 47% inhibition respectively. In addition, the previous compounds also showed increasing in p35 levels to approximately 1.3, 1.5-fold respectively when compared to untreated cells. Flowcytometric cell cycle study using compounds **2d** and **4b** on the wild-type p53-bearing MCF7 breast cancer cell line revealed notable S phase depletion. Our investigations showed that the chalcone-based compounds have the potential to function as anticancer agents. Creating more derivatives would broaden the scope of the SAR analysis and investigate more powerful analogues.

5. Conflicts of interest

The authors declare that they have no conflict of interest.

6. Formatting of funding sources

No funding sources.

7. References

[1] Mabe K, Inoue K, Kamada T, Kato K, Kato M and Haruma K (2022), Endoscopic screening for gastric cancer in Japan: Current status and future perspectives. Digestive Endoscopy 34: p. 412–419.
[2] Ayenigbara IO (2023), Risk-Reducing Measures for Cancer Prevention. Korean Journal of Family Medicine 44: p.76.
[3] WHO Organization (2020), WHO report on cancer: setting priorities, investing wisely and providing care for all. World Health Organization.
[4] Tarin D (2023), Causes of cancer and mechanisms of carcinogenesis, in: Understanding Cancer: The Molecular Mechanisms, Biology, Pathology and Clinical Implications of Malignant Neoplasia. Springer p. 229–279.
[5] Mazingi D, Lakhoo K (2023), Cancer Development and Progression and the "Hallmarks of Cancer," in: Pediatric Surgical Oncology. Springer p. 1–15.
[6] Borrero LJH, El-Deiry WS (2021), Tumor suppressor p53: Biology, signaling pathways, and therapeutic targeting, Biochimica et Biophysica Acta (BBA). Reviews on Cancer 1876: p. 188556.
[7] Catizone AN (2020), The Guardian of the Genome: Regulation of the enhancer networks governing the p53-mediated stress response. State University of New York at Albany.
[8] Kastenhuber ER, Lowe SW (2017), Putting p53 in context. Cell 170: p. 1062–1078.
[9] Levine AJ (2020), p53: 800 million years of evolution and 40 years of discovery. Nature Reviews Cancer 20: p. 471–480.
[10] Pervushin NV, Nilov DK, Pushkarev SV, Shipunova VO, Badlaeva AS, Yapryntseva MA, Kopytova DV, Zhivotovsky B and Kopeina GS (2024), BH3-mimetics or DNA-damaging agents in combination with RG7388 overcome p53 mutation-induced resistance to MDM2 inhibition. Apoptosis 29: p. 2197–2213.
[11] George B, Kantarjian H, Baran N, Krocker JD and Rios A (2021), TP53 in acute myeloid leukemia: molecular aspects and patterns of mutation. International Journal of Molecular Science 22: p. 10782.
[12] Bykov VJN, Eriksson SE, Bianchi J and Wiman KG (2018), Targeting mutant p53 for efficient cancer therapy. Nature Reviews Cancer 18: p. 89–102.
[13] Sullivan KD, Galbraith MD, Andrysik Z and Espinosa JM (2018), Mechanisms of transcriptional regulation by p53. Cell Death Differentiation 25: p. 133–143.
[14] Benedetti R, Crosta MDi, D'Orazi G and Cirone M (2024), Post-Translational Modifications (PTMs) of mutp53 and Epigenetic Changes Induced by mutp53. Biology (Basel) 13: p.508.
[15] Grigoreva TA, Romanova AA, Tribulovich VG, Pestov NB, Oganov RA, Kovaleva DK, Korneenko TV and Barlev NA (2024), p53: The Multifaceted Roles of Covalent Modifications in Cancer. Pharmaceuticals 17: p. 1682.
[16] Masoodi G, Jan N, Jan A and Mir MA (2025), Role of Post-Translational Modifications in the Regulation of Mutant p53, in: P53 in Breast Cancer. CRC Press p. 163–172.
[17] Janic A, Abad E and Amelio I (2025), Decoding p53 tumor suppression: a crosstalk between genomic stability and epigenetic control? Cell Death Differentiation 32: p. 1–8.
[18] Aubrey BJ, Kelly GL, Janic A, Herold MJ and Strasser A (2018), How does p53 induce apoptosis and how does this relate to p53-mediated tumour suppression? Cell Death Differentiation 25: p. 104–113.
[19] Vaddavalli PL, Schumacher B (2022), The p53 network: cellular and systemic DNA damage responses in cancer and aging. Trends in Genetics 38: p. 598–612.
[20] Ma M, Hua S, Min X, Wang L, Li J, Wu P, Liang H, Zhang B, Chen X and Xiang S (2022), p53 positively regulates the proliferation of hepatic progenitor cells promoted by laminin-521. Signal Transduction and Targeted Therapy 7: p. 290.
[21] Abubakar M, Rehman B (2024), Roles of mutant TP53 gene in cancer development and progression. Proceedings of Anticancer Research 8: p. 165–181.
[22] Wang H, Guo M, Wei H and Chen Y (2023), Targeting p53 pathways: Mechanisms, structures and advances in therapy. Signal Transduction Targeted Therapy 8: p. 92.
[23] Loh SN (2021), Arsenic and an old place: rescuing p53 mutants in cancer. Cancer Cell 39: p 140–142.

[24] Olaoba OT, Adelusi TI, Yang M, Maidens T, Kimchi ET, Staveley-O'Carroll KF and Li G (2024), Driver mutations in pancreatic cancer and opportunities for targeted therapy. Cancers (Basel) 16: p. 1808.
[25] Song B, Yang P and Zhang S (2024), Cell fate regulation governed by p53: Friends or reversible foes in cancer therapy. Cancer Communications 44: p. 297–360.
[26] Zhu IY, Lloyd A, Critchley WR, Saikia Q, Jade D, Divan A, Zeqiraj E, Harrison MA, Brown CJ and Ponnambalam S (2025), Structure and function of MDM2 and MDM4 in health and disease. Biochemical Journal 482 (04): p. 241–262.
[27] Ramli I, Cheriet T, Posadino AM, Giordo R, Fenu G, Nwachukwu KC, Oyewole OA, Adetunji CO, Calina D and Sharifi-Rad J (2024), Modulating the p53-MDM2 pathway: the therapeutic potential of natural compounds in cancer treatment. EXCLI Journal 23: p. 1397.
[28] Yao Y, Zhang Q, Li Z and Zhang H (2024), MDM2: current research status and prospects of tumor treatment. Cancer Cell International 24: p. 170.
[29] Huang Y, Che X, Wang PW and Qu X (2024), p53/MDM2 signaling pathway in aging, senescence and tumorigenesis. Seminars in Cancer Biology, Elsevier 101: p. 44-57
[30] Nayak SK, Khatik GL, Narang R, Monga V and Chopra HK (2018), p53-Mdm2 interaction inhibitors as novel nongenotoxic anticancer agents. Current Cancer Drug Targets 18: p. 749–772.
[31] Silva JL, Lima CGS, Rangel LP, Ferretti GDS, Pauli FB, Ribeiro RCB, Silva T B, Silva FC and Ferreira VF (2020), Recent synthetic approaches towards small molecule reactivators of p53. Biomolecules 10: p. 635.
[32] Girgis AS, Zhao Y, Nkosi A, Ismail NSM, Bekheit MS, Aboshouk DR, Aziz MN, Youssef MA and Panda SS (2025), The Therapeutic Potential of Spirooxindoles in Cancer: A Focus on p53–MDM2 Modulation. Pharmaceuticals 18: p. 274.
[33] Alaseem AM (2023), Advancements in MDM2 inhibition: clinical and pre-clinical investigations of combination therapeutic regimens. Saudi Pharmaceutical Journal 31 (10): p. 101790.
[34] Holzer P, Masuya K, Furet P, Kallen J, Valat-Stachyra T, Ferretti S, Berghausen J, Bouisset-Leonard M, Buschmann N and Pissot-Soldermann C (2015), Discovery of a dihydroisoquinolinone derivative (NVP-CGM097): a highly potent and selective MDM2 inhibitor undergoing phase 1 clinical trials in p53wt tumors. Journal of Medicinal Chemistry, 58: p. 6348–6358.
[35] Rew Y, Sun D, Gonzalez-Lopez TF, Bartberger MD, Beck HP, Canon J, Chen A, Chow D, Deignan J and Fox BM (2012), Structure-based design of novel inhibitors of the MDM2–p53 interaction. Journal of Medicinal Chemistry 55: p. 4936–4954.
[36] Bernard D, Zhao Y and Wang S (2012), AM-8553: A Novel MDM2 Inhibitor with a Promising Outlook for Potential Clinical Development. Journal of Medicinal Chemistry 55: p. 4934–4935.
[37] Dziągwa-Becker M, Oleszek M, Zielińska S and Oleszek W (2024), Chalcones—Features, Identification Techniques, Attributes, and Application in Agriculture. Molecules 29: p. 2247.
[38] Akhter F, Marufa SS, Shohag SMAU, Nishino H, Alam MS, Haque MA and Rahman MM (2025), Synthesis, antimicrobial evaluation, ADMET prediction, molecular docking and dynamics studies of pyridine and thiophene moiety-containing chalcones. Royal Society Open Science 12: p. 241411.
[39] Felippe WQ, Barbosa IR, Oliveira AA, Costa GL and Echevarria A (2025), Antifungal effects of thiosemicarbazone-chalcones on Aspergillus, Candida and Sporothrix strains. Achieves of Microbiology 207: p. 1–9.
[40] Gaur R, Jyoti, Khan S, Cheema HS, Khan F, Darokar MP and Bhakuni RS (2024), Synthesis, molecular modelling studies of artemisinin-chalcone derivatives and their antimalarial activity evaluation. Natural Product Research p. 1–11.
[41] Iqtadar R, Naz A, Shah SAA, Ali S and Abdullah S (2025), New halogenated chalcones as potential anti-inflammatory agents: A comprehensive In-Silico, In-Vitro, and In-Vivo study with ADME profiling. Journal of Molecular Structure 1326: p. 141055.
[42] Barreto TSA, Santos TAC, Silva ARST, Costa EV, Pinheiro LA, Fernandes RPM, Scher R and Alves PB (2025), Brominated chalcones as promising antileishmanial agents. Bioorganic and Medicinal Chemistry Letters 116 p. 130042.
[43] Priya S, Islam MM, Kasana S, Kurmi B, Gupta G and Patel P (2025), Therapeutic potential of chalcone-1, 2, 3-triazole hybrids as anti-tumour agents: a systematic review and SAR studies. Future Medicinal Chemistry 17(4): p. 449–465.
[44] Dadou S, Altay A, Baydere C, Anouar EH, Türkmenoğlu B, Koudad M, Dege N, Oussaid A, Benchat N and Karrouchi K (2025), Chalcone-based imidazo [2, 1-b] thiazole derivatives: synthesis, crystal structure, potent anticancer activity, and computational studies. Journal of Biomolecular Structure Dynamics 43: p. 261–276.
[45] Zhang C, Liu Y, Zhang X, Wan C and Mao Z (2025), Synthesis and anti-tumor activity of new benzofuran-based chalcone derivatives as potent VEGFR-2 inhibitors. RSC Medicinal Chemistry 16: p. 392–399.
[46] Das M, Manna K (2016), Chalcone scaffold in anticancer armamentarium: a molecular insight. Journal of Toxicology 2016: p. 7651047.
[47] Mahapatra DK, Bharti SK and Asati V (2015), Anti-cancer chalcones: Structural and molecular target perspectives. European Journal of Medicinal Chemistry 98: p. 69–114.
[48] Mahapatra DK, Bharti SK and Asati V (2015), Chalcone scaffolds as anti-infective agents: Structural and molecular target perspectives. European Journal of Medicinal Chemistry 101: p. 496–524.
[49] Mohamed MF, Hassaneen HM and Abdelhamid IA (2018), Cytotoxicity, molecular modeling, cell cycle arrest, and apoptotic induction induced by novel tetrahydro-[1, 2, 4] triazolo [3, 4-a] isoquinoline chalcones. European Journal of Medicinal Chemistry 143: p. 532–541.
[50] Chaithanya B, Chary DP and Rao AV (2024), Synthesis and Biological Evaluation of chalcone Incorporated thaizole-isoxazole Derivatives as Anticancer Agents. Chemical Data Collections 55: p. 101177.

[51] Kasetti AB, Singhvi I, Nagasuri R, Bhandare RR and Shaik AB (2021), Thiazole–chalcone hybrids as prospective antitubercular and antiproliferative agents: Design, synthesis, biological, molecular docking studies and in silico ADME evaluation. Molecules 26: p. 2847.
[52] Xu F, Li W, Shuai W, Yang L, Bi Y, Ma C, Yao H, Xu S, Zhu Z and Xu J (2019), Design, synthesis and biological evaluation of pyridine-chalcone derivatives as novel microtubule-destabilizing agents. European Journal of Medicinal Chemistry 173: p. 1–14.
[53] Elkhalifa D, Siddique AB, Qusa M, Cyprian FS, El Sayed K, Alali F, Al Moustafa AE and Khalil A (2020), Design, synthesis, and validation of novel nitrogen-based chalcone analogs against triple negative breast cancer. European Journal of Medicinal Chemistry 187: p. 111954.
[54] Stoll R, Renner C, Hansen S, Palme S, Klein C, Belling A, Zeslawski W, Kamionka M, Rehm T and Mühlhahn P (2001), Chalcone derivatives antagonize interactions between the human oncoprotein MDM2 and p53. Biochemistry 40: p. 336–344.
[55] Beloglazkina A, Zyk N, Majouga A and Beloglazkina E (2020), Recent small-molecule inhibitors of the p53–MDM2 protein–protein interaction. Molecules 25: p. 1211.
[56] Iftikhar S, Khan S, Bilal A, Manzoor S, Abdullah M, Emwas AH, Sioud S, Gao X, Chotana GA and Faisal A (2017), Synthesis and evaluation of modified chalcone based p53 stabilizing agents. Bioorganic Medicinal Chemistry Letters 27: p. 4101–4106.
[57] Hsu YL, Kuo PL, Lin LT and Lin CC (2005), Isoliquiritigenin inhibits cell proliferation and induces apoptosis in human hepatoma cells. Planta Medica 71: p. 130–134.
[58] Mukhtar SS, Morsy NM, Hassan AS, Hafez TS, Hassaneen HM and Saleh FM (2022), A review of chalcones: synthesis, reactions, and biological importance. Egyptian Journal of Chemistry 65: p. 379–395.
[59] Liu Z, Zeng L, Wu L, Song D and Chen Y (2025), Facile synthesis of thiophene-embedded Baicalein via oxidative cyclization and anticancer activity against ovarian cancer cells via inhibiting PI3K/MTOR signaling pathway: in-vitro and in-silico study. Bulletin of the Chemical Society Ethiopia 39: p. 367–379.
[60] Leonte D, Coman F, Fotso GW, Ngadjui BT, Zaharia V and Ngameni B (2021), Heterocycles 49. Synthesis, Chemical Behaviour and Biological Properties of Heterocyclic Chalcones. Review from our Research. Farmacia 69: p. 821-836
[61] Pischetola C, Ruiz-Ruiz A and Cárdenas-Lizana F (2021), Continuous production of benzylideneacetophenone via gas phase reaction of benzaldehyde and acetophenone: Mechanism and reaction kinetics. Chemical Engineering Journal 418: p. 129306.
[62] Silva WA, Nogueira FM and Takada SCS (2024), Claisen-Schmidt condensation: an interdisciplinary journey in the organic synthesis laboratory. Chem Rxiv p. 1-21.
[63] Ghasemi M, Turnbull T, Sebastian S and Kempson I (2021), The MTT assay: utility, limitations, pitfalls, and interpretation in bulk and single-cell analysis. International Journal of Molecular Sciences 22: p. 12827.
[64] Popov AB, Krstulović L, Koštrun S, Jelić D, Bokulić A, Stojković MR, Zonjić I, Taylor MC, Kelly JM and Bajić M (2020), Design, synthesis, antitrypanosomal activity, DNA/RNA binding and in vitro ADME profiling of novel imidazoline-substituted 2-arylbenzimidazoles. European Journal of Medicinal Chemistry 207: p. 112802.
[65] Abdullah MN, Osw P, Hassan SA and Othman S (2024), Two new cyclohexenone derivatives: Synthesis, DFT estimation, biological activities and molecular docking study. Journal of Molecular Structure 1301: p. 137361.
[66] Arora V, Arora P and Lamba H (2012), Synthesis and biological activities of some 3, 5-disubstituted pyrazoline derivatives of 2-acetyl naphthalene. International Journal of Pharmacy and Pharmaceutical Sciences 4: p. 303-306.
[67] Kaul S, Hooda K, Chatterjee M, Jan A and Mir MA (2025), Targeted Therapies against Mutated p53 in Breast Cancer, P53 in Breast Cancer. CRC Press p. 200–211.
[68] Matthews HK, Bertoli C and Bruin RAM (2022), Cell cycle control in cancer. Nature Reviews Molecular Cell Biology 23: p. 74–88.